

First-principles approach to phase stability for a ternary σ phase: Application to Cr-Ni-ReMauro Palumbo,^{1,2} Taichi Abe,² Suzana G. Fries,¹ and Alain Pasturel³¹ICAMS, Ruhr University Bochum, Stiepelers Straße 129, D-44801 Bochum, Germany²NIMS, National Institute for Materials Science, 1-2-1 Sengen, Tsukuba, Ibaraki 305-0047, Japan³SIMAP, UMR CNRS-INPG-UJF 5266, BP 75, F-38402 Saint Martin d'Hères, France

(Received 30 November 2010; revised manuscript received 1 February 2011; published 21 April 2011)

First-principles calculations of formation energies for 243 different configurations of the Cr-Ni-Re σ phase were used to calculate a ternary phase diagram in the Bragg-Williams-Gorsky approximation (BWG) and to model finite-temperature thermodynamic properties. The binary and ternary phase diagrams were then calculated at different temperatures. Correct topology of the experimental ternary isothermal section of the phase diagram has been obtained with a relatively small difference in temperature between calculations and experiments.

DOI: [10.1103/PhysRevB.83.144109](https://doi.org/10.1103/PhysRevB.83.144109)

PACS number(s): 61.66.Dk, 81.30.Bx, 64.60.Bd, 82.60.Lf

I. INTRODUCTION

The σ phase is brittle and its occurrence in highly alloyed steels and Ni-based superalloys can strongly degrade their mechanical properties. For this reason, this phase has been the subject of several theoretical investigations in the literature, some of them being reported in Refs. 1–9. All these works deal with binary σ phases. First-principles calculations at 0 K, the Connolly-Williams method (CWM),¹⁰ and the cluster variation method (CVM)¹¹ were used in Refs. 1–3 for the calculation of site occupancies as functions of temperature and composition in different binary systems. It was also shown that the compound energy formalism (CEF), which is based on a generalized Bragg-Williams-Gorsky approximation (BWG) ignoring short-range order, can provide satisfactory results for the calculation of site fractions.^{5,6,9} Phase diagrams calculated with these methods can even produce the same topology as experimental ones.⁹ Very recently, the ternary Cr-Mo-Re sigma phase was investigated by first-principles calculations and site occupancies were calculated in the BWG approximation.¹² The Re preference for high coordination number sites in Cr-Re¹³ and low coordination number sites in Mo-Re¹² was correctly predicted, but no attempt was made to calculate first-principles phase diagrams. To the best of the authors' knowledge, ternary phase diagrams with only fcc or bcc solid solutions were attempted in the past by first-principles calculations^{14–16} or were limited to pseudobinary sections of ternary systems.^{17–20}

In this work, we investigate the Cr-Ni-Re system where the σ phase is the only intermetallic stable phase in the ternary experimental phase diagram. First-principles calculations of formation energies for 243 different configurations of the Cr-Ni-Re σ phase were carried out and were used in the Bragg-Williams-Gorsky approximation (BWG) to model finite-temperature thermodynamic properties. A ternary phase diagram, including the σ phase, was then calculated for the first time without any fitting parameters. The present approach can also be extended to higher order systems.

II. MODELING AND METHODOLOGY

First-principles calculations were performed using density functional theory (DFT) as implemented in the Vienna

Ab initio Simulation Package (VASP) with plane wave basis sets.^{21–23} The calculations employed the generalized gradient approximation (GGA-PW91) of Perdew and Wang,²⁴ the valence electrons were explicitly represented with projector augmented wave (PAW) pseudopotentials, and the k -point meshes were created using the Monkhorst-Pack scheme.²⁵ The recommended standard pseudopotentials provided within the VASP package were used for Cr, Ni, and Re (6 or 7 valence electrons).²⁶ The ground state (0 K) structure was determined by minimizing the Hellmann-Feynman forces using the conjugate gradient algorithm, until all ionic forces were found to be less than 0.02 eV/Å. The setting “Precision=Accurate” option in VASP was used. Several relaxation steps were performed, both for internal atomic coordinates and lattice parameters, but keeping the tetragonal cell structure. A final static calculation was then performed using the linear tetrahedron method with Blochl corrections²⁷ for accurate integration in the reciprocal space. For the sigma phase, the plane wave cutoff energy was set to 350 eV with a 126 irreducible k -point mesh. For the bcc Cr, fcc Ni, and hcp Re, the cutoff energy was set to 350 eV with a 28*28*28 k -point mesh. The energy of formation E_{ijklm} for each $ijklm$ configuration in the thermodynamic modeling of the sigma phase, where i, j, k, l, m can be Cr, Ni, or Re, was obtained from the following equation:

$$E_{ijklm} = E_{ijklm} - xE_{Cr,bcc} - yE_{Ni,fcc} - zE_{Re,hcp}, \quad (1)$$

where E_{ijklm} , $E_{Cr,bcc}$, $E_{Ni,fcc}$, and $E_{Re,hcp}$ are the total energies for the $ijklm$ configuration, pure bcc Cr, pure fcc Ni, and pure hcp Re, respectively. In addition, x , y , and z are the mole fractions of Cr, Ni, and Re. At 0 K and after full relaxation ($P = 0$) this corresponds to the enthalpy of formation. Harmonic and anharmonic contributions at higher temperatures were neglected in the present calculations. For magnetic effects, collinear magnetic configurations were considered, and spin flips were allowed. Ferromagnetic and antiferromagnetic ground state configurations were also considered for the sigma phase, which is further discussed in the following sections.

The thermodynamic stability of any solid phase at $T \neq 0$ K is governed by the Gibbs energy

$$G = E + PV - TS. \quad (2)$$

The PV term can be neglected in the present considerations. The entropy term is generally both configurational and vibrational. The vibrational contribution can be important or negligible depending on the type of solid phase considered.²⁸

III. RESULTS AND DISCUSSION

Results for the energy of formation at 0 K of all the ternary configurations in the σ phase calculated by first principles are reported as supplementary material.²⁹ Calculated magnetization, lattice parameters, cell volume, and c/a ratio are also reported in the table provided as supplementary material.²⁹

The σ phase ($D8_b$) is an intermetallic phase of the group of Frank-Kasper phases,^{30,31} also known as topologically close packed (tcp) phases. Recently, an extended review on the σ phase was published.³² The crystal structure is tetragonal, described by the $P4_2/mnm$ space group (Table 1), with five nonequivalent positions ($2a$, $4f$, $8i_1$, $8i_2$, $8j$), which present coordination numbers of 12, 15, 14, 12, and 14, respectively (Fig. 1 and Table I). These five nonequivalent sites generate $2^5 = 32$ ordered configurations in a binary system, and $3^5 = 243$ configurations in a ternary system. Because of the same multiplicity (8) of Wyckoff sites $8i_1$, $8i_2$, $8j$, several configurations yield the same composition by atom permutation. Thus, the 32 (243) configurations in a binary (ternary) system give rise to 16 (90) different unique compositions.

Almost all calculated DFT energies for these configurations are positive (reference states are bcc Cr, fcc Ni, and hcp Re), except for three configurations (Cr at $2a$ Re at $4f$ Re at $8i_1$ Ni at $8i_2$ Cr at $8j$, Ni at $2a$ Re at $4f$ Re at $8i_1$ Ni at $8i_2$ Cr at $8j$, Re at $2a$ Re at $4f$, Re at $8i_1$ Ni at $8i_2$ Cr at $8j$) whose compositions are $\text{Cr}_{33}\text{Ni}_{27}\text{Re}_{40}$, $\text{Cr}_{27}\text{Ni}_{33}\text{Re}_{40}$, and $\text{Cr}_{26}\text{Ni}_{27}\text{Re}_{47}$, respectively. It is very interesting that these configurations differ only for the atom occupying the first Wyckoff position ($2a$) and they are close in composition.

In several binary systems, it has been observed that the most stable composition for the sigma phase corresponds to an A_2B stoichiometry. Typically, A is an element with a large atomic radius and a bcc crystal structure, is poor in d electrons, and shows a preference for high coordination sites ($4f$, $8i_1$, $8j$), while B has a small atomic radius and an fcc or hcp crystal structure, is rich in d electrons, and shows a preference for low coordination sites ($2a$, $8i_2$).³⁰⁻³² A general explanation for the stability of A_2B stoichiometry is based on atomic size arguments, when the A atoms occupy $4f$, $8i_1$, $8j$ sites (two-thirds of the total) and B atoms occupy $2a$, $8i_2$ (one-third of the total). However, many exceptions to this simple scheme

TABLE I. Crystal structure of the σ -phase: Sites, Wyckoff position, atomic positions (average values) in the $P4_2/mnm$ (No. 136) space group, and coordination number (Ref. 32).

Sublattice	Wyckoff	x	y	z	CN
1	$2a$	0	0	0	12
2	$4f$	$\simeq 0.399$	x	0	15
3	$8i_1$	$\simeq 0.464$	$\simeq 0.131$	0	14
4	$8i_2$	$\simeq 0.741$	$\simeq 0.066$	0	12
5	$8j$	$\simeq 0.187$	x	$\simeq 0.251$	14

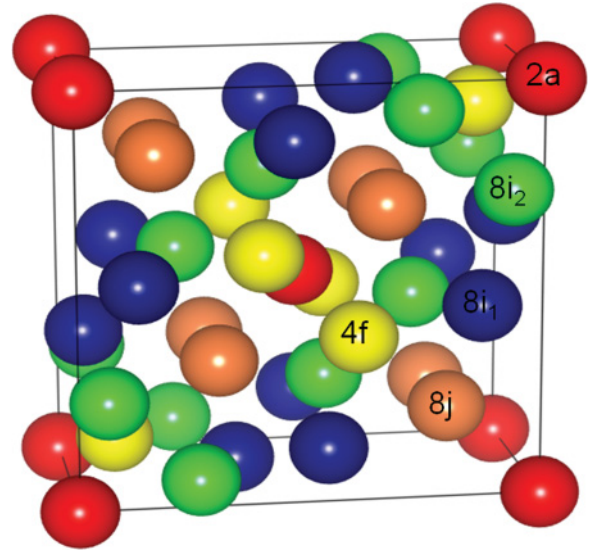


FIG. 1. (Color online) Crystal structure of sigma phase.

have been found,^{3,32} but also confirmation in other cases.⁷ An alternative definition of A and B elements was also proposed,³² based only on the site occupancy preference, where A is the element which shows a preference for high coordination number sites. In the ternary case, the classification of an element as A or B is not straightforward whatever definition is applied. Nonetheless, the most stable ternary compositions do not completely fulfill this rule, whatever atom is considered as A or B (Table II), and this interpretation scheme seems too simple for the present case. Besides, the definition of A -type and B -type atoms is even less well defined in the ternary case. More complex approaches have been proposed recently,³³ in which correlations between parameters such as atomic volumes, average electronic density, and stability range for several tcp phases were tested.

By examining the configurations which are close in composition to the most stable ones, one can notice that along lines with constant Cr and Ni composition the energy does not show a significant change, while the change is more abrupt considering the line with constant Re composition. Moreover the calculated DFT volumes along the two isocomposition sections with constant Cr and Ni content closely follow Vegard's law (Fig. 2). The calculated volume for configuration No. 115 in the supplementary material²⁹ ($V = 0.381 \text{ nm}^3$) compares well with the only experimental value available for the ternary σ phase ($V = 0.386 \text{ nm}^3$),³⁴ and the lattice parameters compare equally well (calc. $a = 0.9138 \text{ nm}$, $c = 0.4565 \text{ nm}$; exp. $a = 0.9071 \text{ nm}$, $c = 0.4692 \text{ nm}$).

TABLE II. Stoichiometry of the most stable ternary configurations according to different A/B classification of the elements (see text for details).

A Elements	B Elements	Most Stable Stoichiometries
Cr, Ni	Re	$A_{60}B_{40}$, $A_{60}B_{40}$, $A_{53}B_{47}$
Cr, Re	Ni	$A_{73}B_{27}$, $A_{67}B_{33}$, $A_{73}B_{27}$
Ni, Re	Cr	$A_{67}B_{33}$, $A_{73}B_{27}$, $A_{73}B_{27}$

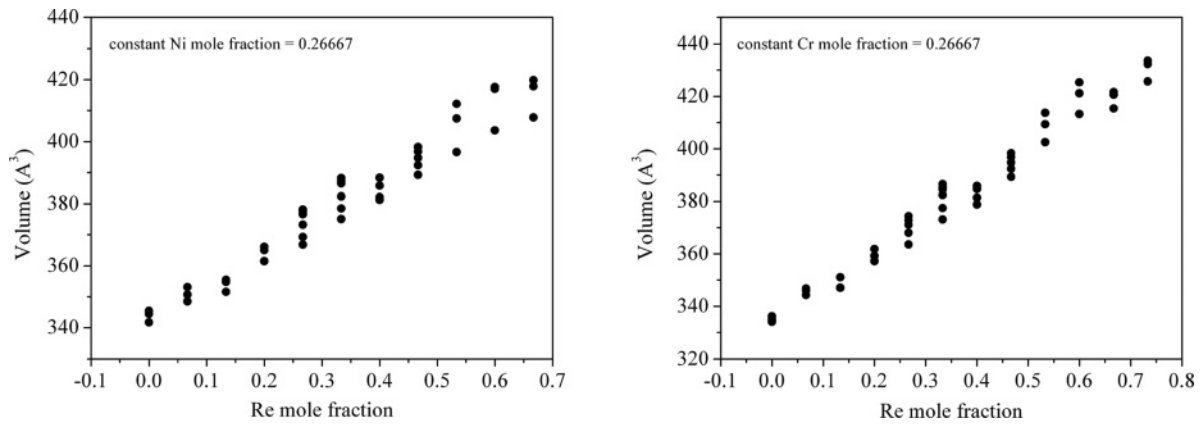


FIG. 2. Calculated DFT volumes of different σ -phase configurations along different sections of the ternary composition space.

The calculated energies at 0 K for the binary subsystems are shown in Fig. 3. All energies are positive in the binary systems; i.e., the σ phase is not stable at 0 K. The magnetization is negligible for most configurations (see supplementary material²⁹), but in a few Ni-rich ones magnetism significantly affects the calculated energies. As expected, the effect is

maximum when all sites are occupied by Ni atoms. For the σ phase, the successful application of the Bragg-Williams-Gorsky approximation suggests that vibrational contributions are negligible.^{5,6}

The Bragg-Williams-Gorsky approximation was thus applied using the CEF formalism.³⁵ A five-sublattice model

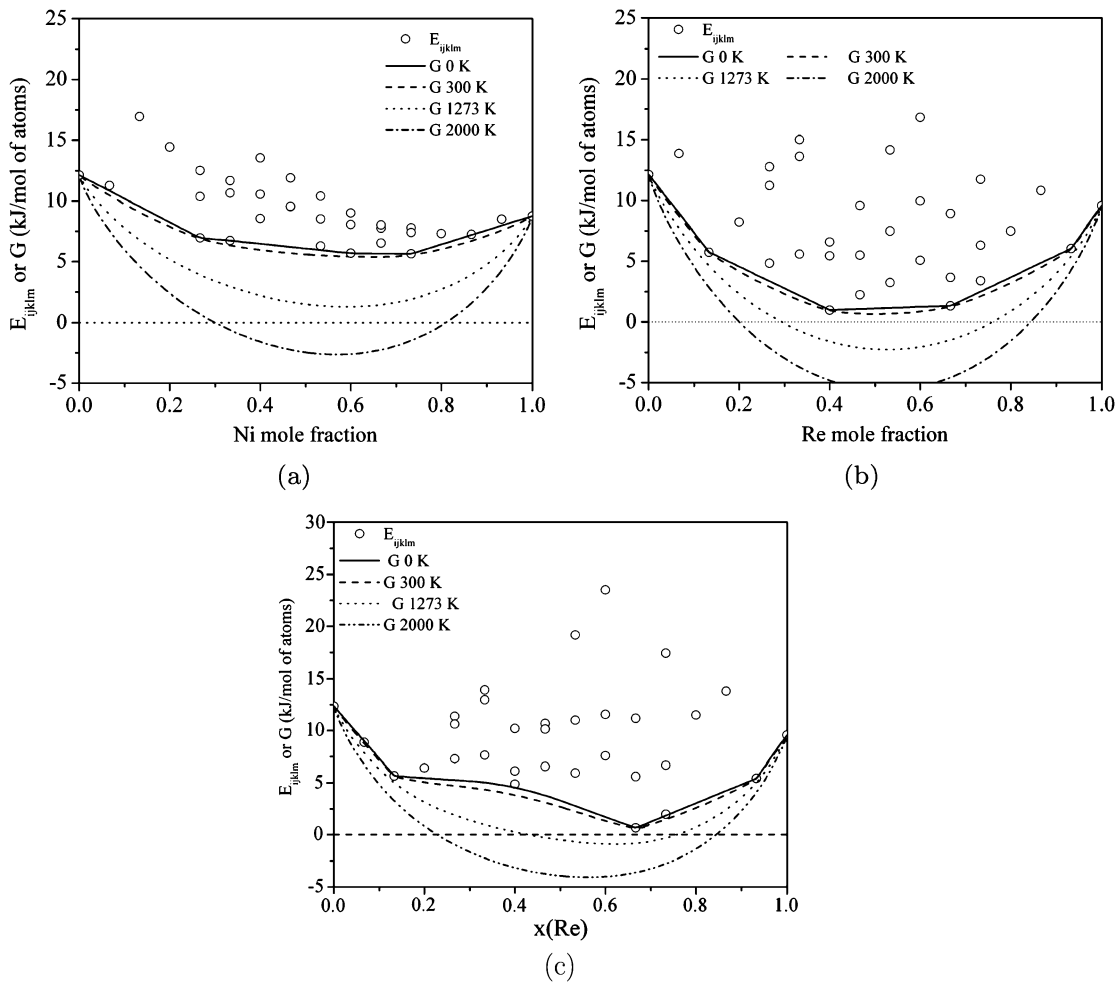


FIG. 3. Calculated first-principles enthalpies of formation at 0 K of the 32 end members of the sigma phase (open circle markers) and Gibbs free energy at different temperatures calculated using the CEF within the five-sublattice model (lines). Reference states are the bcc Cr, Ni fcc, and hcp Re. (a) The Cr-Ni system. (b) The Cr-Re system. (c) The Ni-Re system.

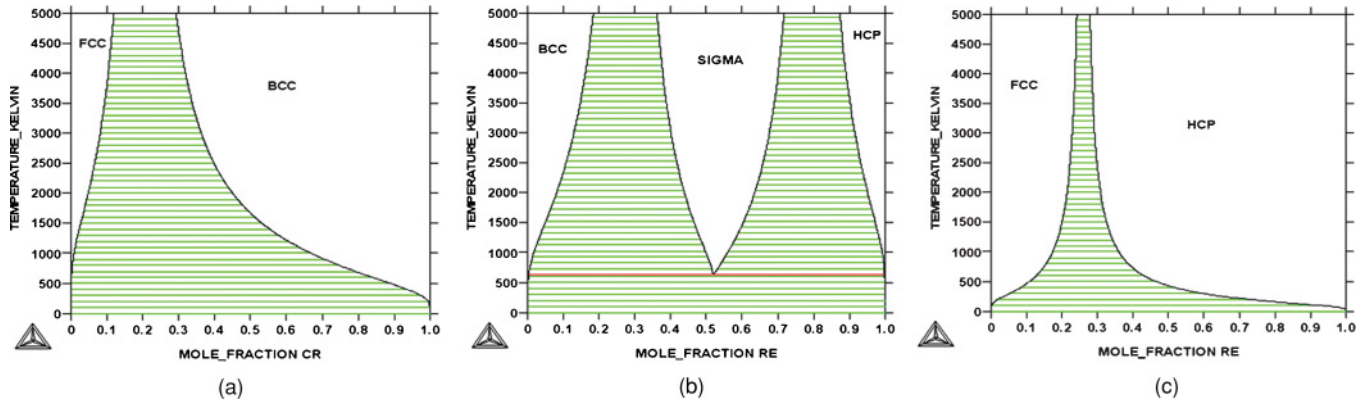


FIG. 4. (Color online) Calculated binary phase diagrams. (a) The Ni-Cr phase diagram. (b) The Cr-Re phase diagram. (c) The Ni-Re phase diagram.

$(\text{Cr,Ni,Re})_2(\text{Cr,Ni,Re})_4(\text{Cr,Ni,Re})_8(\text{Cr,Ni,Re})_8(\text{Cr,Ni,Re})_8$ for the σ phase provides the most accurate description of this phase.^{7,13} According to this formalism, the general Gibbs energy expression is

$$G_m = E_m^{\text{srf}} - T S_m^{\text{conf}}. \quad (3)$$

The surface of reference for the model is the sum of total energies of all configurations with atom i on each sublattice s , weighted by the site fractions $y_i^{(s)}$. The corresponding surface energy of reference E^{srf} and configurational entropy S^{conf} are given by

$$E^{\text{srf}} = \sum_{i,j,k,l,m} y_i^{(1)} y_j^{(2)} y_k^{(3)} y_l^{(4)} y_m^{(5)} {}^o E_{ijklm}, \quad (4)$$

$$S^{\text{conf}} = -R \sum_s a^{(s)} \sum_{i=\text{Cr,Ni,Re}} y_i^{(s)} \ln(y_i^{(s)}),$$

where $a^{(s)}$ is the number of sites on sublattice s . The compound energies ${}^o E_{ijklm}$ are obtained by first-principles calculations of the formation enthalpies at 0 K. This means one can directly calculate the properties of the σ -phase in CEF from the first-principles results. No pair- or higher-order effective cluster interaction (ECI) parameters¹⁰ and no fitting parameters are needed to obtain temperature dependent properties. Besides the σ phase, solid solutions bcc, fcc, and hcp are present in the

ternary Cr-Ni-Re phase diagram. They were assumed to have an ideal mixing behavior and their energies were also obtained by first-principles calculations. Thermodynamic properties, site occupancies, and phase diagrams were then calculated using the Thermo-Calc software package version S.³⁶

According to the CEF, the Gibbs energy of the σ phase in the binary systems is calculated at different temperatures and also reported in Fig. 3. As expected, at 0 K the convex hull passing through the most stable enthalpies of formation is obtained, while the entropic contribution in the BWG leads to a negative value of the Gibbs energy at high temperatures. Interestingly, a miscibility gap is found at low temperatures in the Ni-Re system according to the CEF model. This feature is extremely difficult to verify experimentally, because the σ phase is not stable at these temperatures and demixing would be very sluggish even at higher temperatures.

Binary phase diagrams were then calculated and are shown in Fig. 4. As can be seen, the σ phase is stable only in the Cr-Re system above $T = 629$ K, in agreement with experimental phase diagrams (see Fig. 5). The low-temperature decomposition of the σ phase is in very good agreement with the CALPHAD-type assessments from Refs. 13 and 41 which are based on parameter-fitting evaluations. In both the Cr-Ni and the Ni-Re systems, only solid-solution phases appear stable. The topology of the calculated phase diagrams compares well with the experimental ones. No liquid phase is modeled;

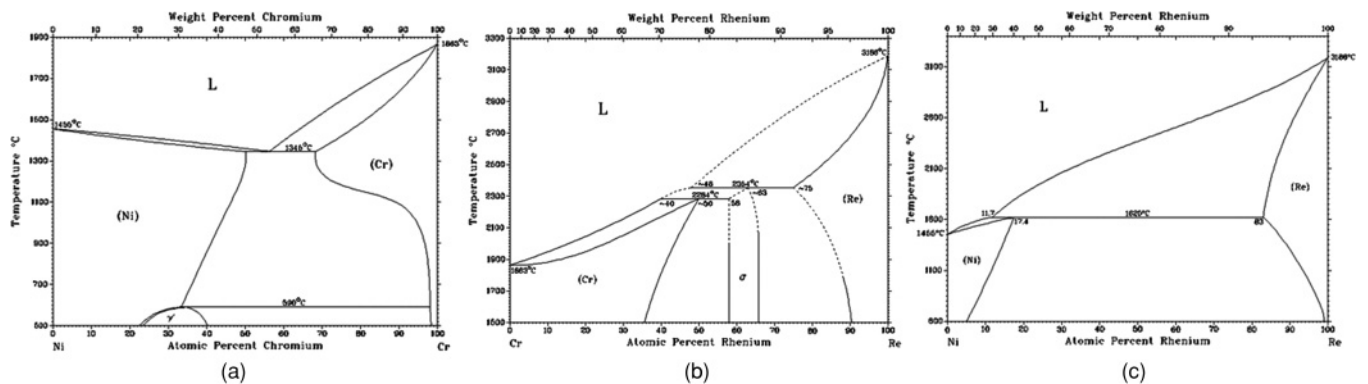


FIG. 5. Experimental binary phase diagrams (from Ref. 37). (a) The Cr-Ni phase diagram. (b) The Cr-Re phase diagram. (c) The Ni-Re phase diagram.

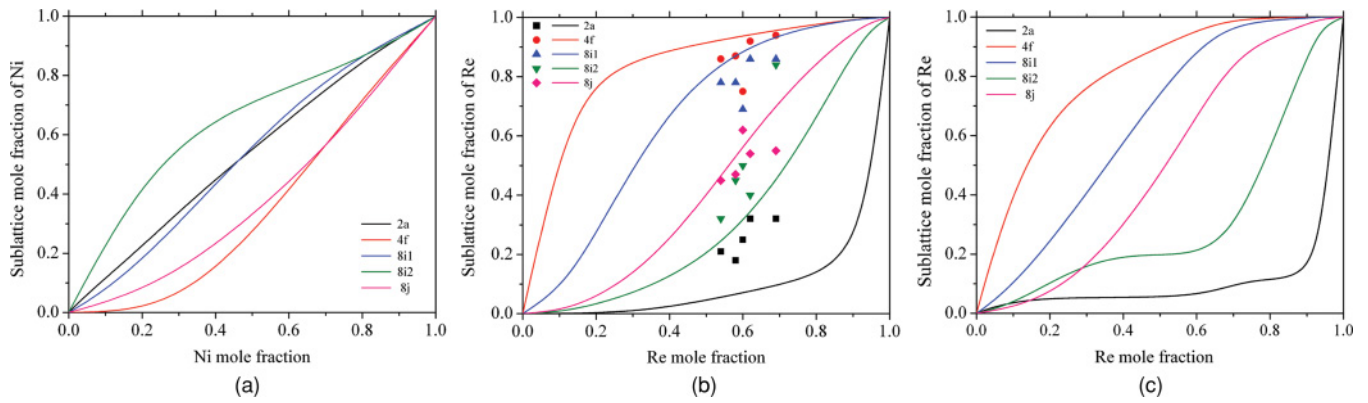


FIG. 6. (Color online) Calculated site occupancy as a function of Ni or Re content in binary subsystems obtained using the CEF model at 1273 K (lines). Experimental data in the Cr-Re system from Ref. 32 and references therein are also plotted for comparison (points). (a) The Cr-Ni system. (b) The Cr-Re system. (c) The Ni-Re system.

thus it does not appear at high temperatures. Besides, the orthorhombic Ni_2Cr (γ') phase, stable only at low temperature, was not included in the present modeling.

Within the Bragg-Williams-Gorsky approximation, site occupancies in the σ phase at different temperatures and compositions can be calculated. Results using the CEF have been found to be comparable at high temperatures (≥ 500 K) with calculations carried out using the cluster expansion-cluster variation method.⁵ Calculated site occupancies in the binary subsystems are reported in Fig. 6. As an example, site occupancies in the Cr-Re system, where experimental data for comparison are available, are reported in Fig. 6(b) and were already discussed in Ref. 13. These results confirm the validity of the CEF and first-principles energies to predict the site preference of Re in different systems. In the Cr-Re

system, Re atoms show a preference for high coordination number (CN) sites (site 4f, CN 15) in agreement with experiments. Re atoms show also the same preference for high CN sites in the Ni-Re system, in contrast to what is observed in other systems (i.e., Mo-Re).³² In the Cr-Ni system, Ni atoms show a slight preference for low coordination number sites but the difference in site preference between Cr and Ni atoms appears less pronounced than in the other binary systems. Site occupancies can also be calculated along sections of the ternary composition space. In the Cr-Mo-Re system, Re atoms show a preference for high CN sites in the Cr-Re binary and for low CN sites in the Mo-Re system. Ternary site occupancies calculated with the present approach along different sections with constant Ni/Re ratio showed a progressive transition from one behavior to the other.¹² In the

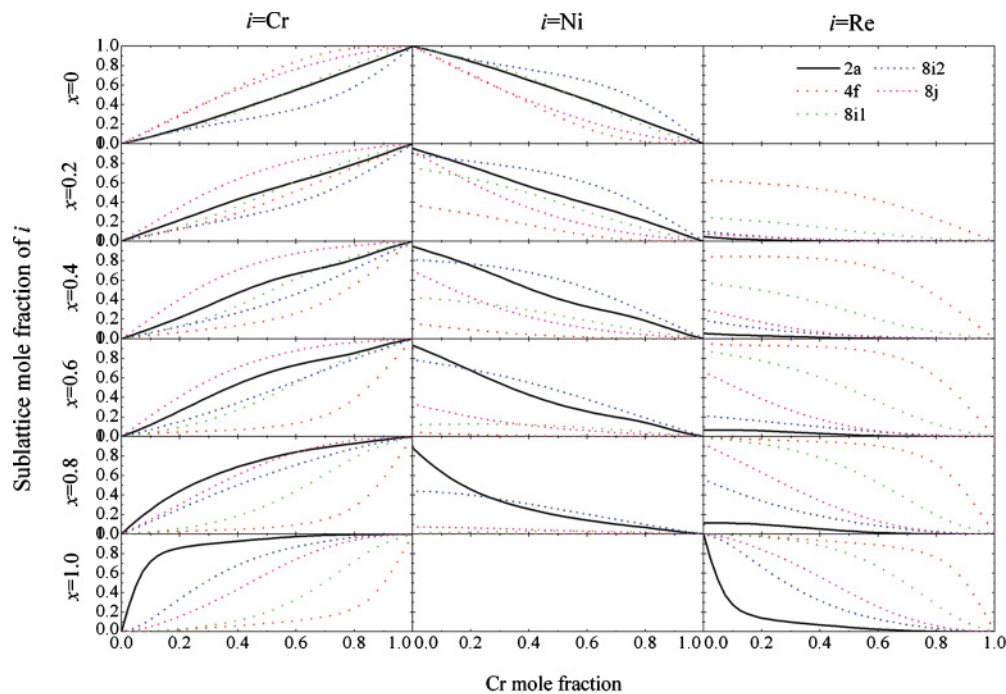


FIG. 7. (Color online) Calculated site occupancy in the sigma phase as a function of Cr content obtained using the CEF model at 1273 K along different sections of the ternary composition space $Cr(Ni_{1-x}Re_x)$.

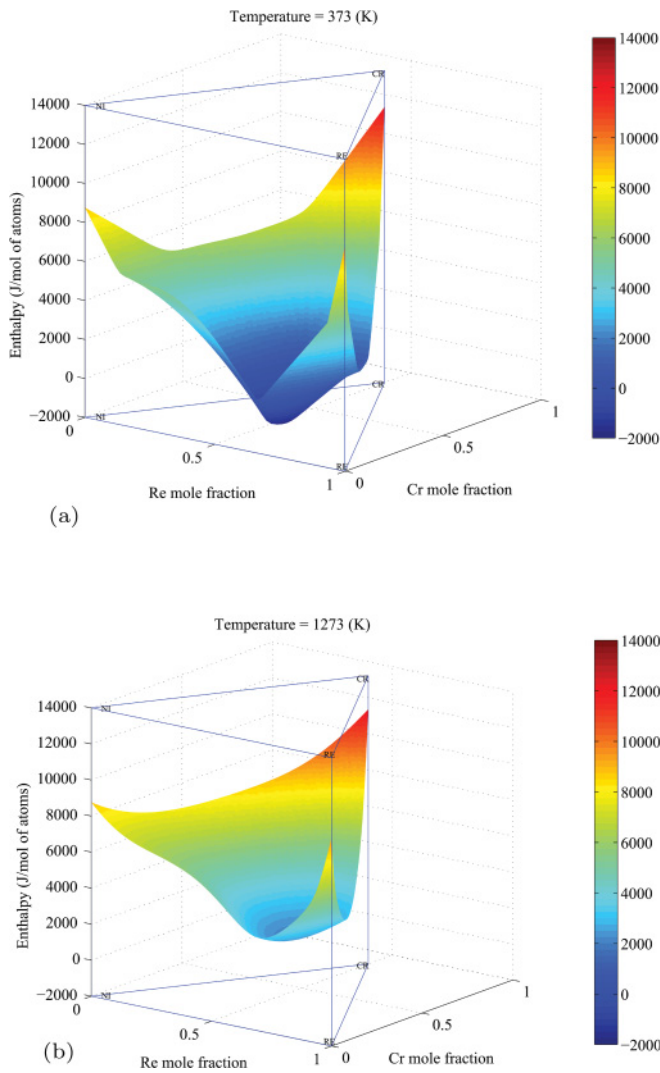


FIG. 8. (Color online) Calculated first-principles enthalpies of formation surface at different temperatures. Reference states are the bcc Cr, Ni fcc, and hcp Re. (a) Calculated enthalpy of the ternary σ phase at 373 K. (b) Calculated enthalpy of the ternary σ phase at 1273 K.

present ternary system, Re shows the same preference for high CN sites in both binary systems and along ternary sections. On the contrary, Cr atoms prefer high CN sites in the Cr-Ni system but low CN sites in the Cr-Re system. The transition from one behavior to the other is shown in Fig. 7. Unfortunately, no ternary experimental data are available for site occupancies.

The calculated enthalpy of the ternary σ phase is shown at $T = 1273$ K in Fig. 8(b). A ternary minimum can be seen, which is even more pronounced at low temperatures [Fig. 8(a)]. The enthalpy becomes smoother increasing the temperature. It is interesting to point out that the enthalpy of the σ phase has a temperature dependence which is not explicitly evident from Eqs. (3) and (4). In fact, the temperature dependence of the enthalpy is due to the change in the site fractions in these equations as a function of temperature, which in turn are obtained by minimization of the Gibbs energy (including the temperature dependent configurational entropy).

The isothermal section at 1423 K of the ternary diagram calculated in the Bragg-Williams-Gorsky approximation is reported in Fig. 9(a). Some experimental data are available for this system at 1423 and 1473 K and are shown for comparison in Fig. 9(b). As can be noticed, in agreement with the experimental phase diagram, the σ phase is stable in the binary Cr-Re side and extends from the binary side to ternary compositions. However, contrary to the experimental evidence, the σ phase is not in equilibrium with the fcc phase, but only with bcc and hcp phases. The calculated isothermal section at 2000 K [Fig. 9(c)] shows that in this case the main topological features of the experimental isothermal section are reproduced by the calculated section, even if the temperature is not the same as in the experimental section. By further increasing the temperature, the isothermal section resembles even closer the experimental one, suggesting that inclusion of vibrational effects could improve the present results. The range of solubility of bcc and fcc solid solutions appears to be underestimated by present calculations, while the hcp phase shows a too large stability range on the binary Ni-Re side.

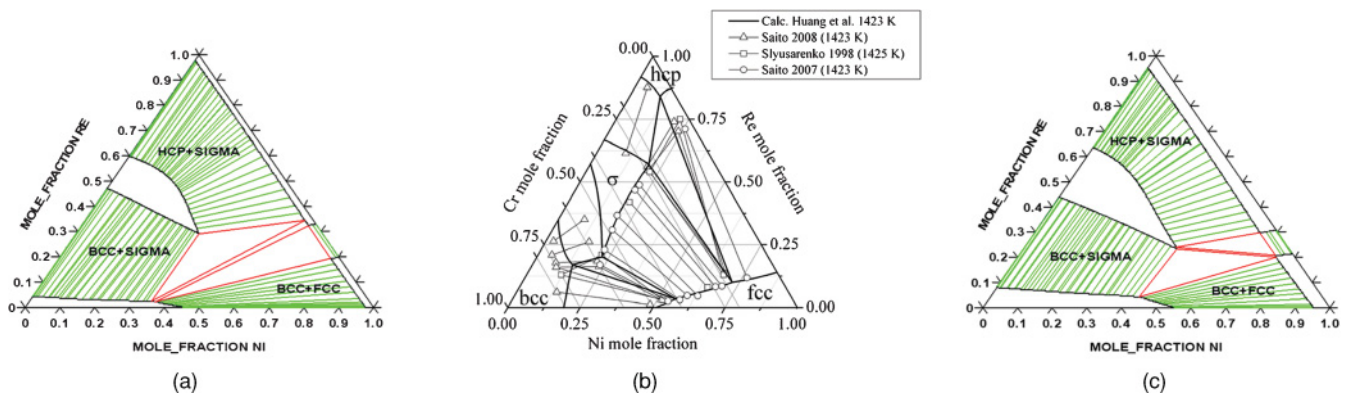


FIG. 9. (Color online) The ternary Cr-Ni-Re phase diagram. (a) Calculated isothermal section of the ternary phase diagram at 1423 K. (b) Experimental isothermal section at 1423 K. Experimental data are from Ref. 38 (Saito 2008), Ref. 39 (Saito 2007), and Ref. 40 (Slyusarenko 1998). Calculations are from Ref. 41 (Huang *et al.*). (c) Calculated isothermal section of the ternary phase diagram at 2000 K.

IV. CONCLUSIONS AND PERSPECTIVES

A thermodynamic description of the ternary Cr-Ni-Re system was achieved by first-principles calculations within the Bragg-Williams-Gorsky approximation. The energies of formation of all 243 possible configurations in the ternary σ phase were computed by VASP at 0 K. Thermodynamic properties at any temperature were then evaluated in the BWG, including the bcc, fcc, and hcp solid solutions. The main result is that some ternary configurations have been found to have negative energy of formation and are stabilized by ternary effects. A miscibility gap was found in the binary Ni-Re

system in the σ phase at low temperatures, which is difficult to confirm experimentally since this phase is not stable under these conditions.

Binary and ternary phase diagrams were calculated with no fitting parameters and they correctly describe the main topological features of the experimental phase diagrams.

The present approach appears to be more feasible for extending to higher order systems at a reasonable computational effort than the cluster expansion and cluster variation methods. Work to include a better description of configurational disorder in the solid solutions and vibrational contributions is ongoing.

-
- ¹M. H. F. Sluiter, K. Esfarjani, and Y. Kawazoe, *Phys. Rev. Lett.* **75**, 3142 (1995).
- ²C. Berne, M. Sluiter, Y. Kawazoe, T. Hansen, and A. Pasturel, *Phys. Rev. B* **64**, 144103 (2001).
- ³M. H. F. Sluiter and A. Pasturel, *Phys. Rev. B* **80**, 134122 (2009).
- ⁴M. H. F. Sluiter, A. Pasturel, and Y. Kawazoe, *Prediction of Site Preference and Phase Stability of Transition Metal Based Frank-Kasper Phases in the Science of Complex Alloy Phases*, edited by P. E. A. Turchi and T. Massalski (TMS, Warrendale, 2005), p. 409.
- ⁵S. G. Fries and B. Sundman, *Phys. Rev. B* **66**, 012203 (2002).
- ⁶P. A. Korzhavyi, B. Sundman, M. Selleby, and B. Johansson, *Mater. Res. Soc. Symp. Proc.* **842**, 517 (2005).
- ⁷O. Grånas, P. A. Korzhavyi, A. E. Kissavos, and I. A. Abrikosov, *CALPHAD* **32**, 171 (2008).
- ⁸J. Pavlů, J. Vřešitál, and M. Šob, *Intermetallics* **18**, 212 (2010).
- ⁹J.-C. Crivello and J.-M. Joubert, *J. Phys. Condens. Matter* **22**, 035402 (2010).
- ¹⁰J. W. D. Connolly and A. R. Williams, *Phys. Rev. B* **27**, 5169 (1983).
- ¹¹R. Kikuchi, *Phys. Rev.* **81**, 998 (1951).
- ¹²J.-C. Crivello, M. Palumbo, T. Abe, and J.-M. Joubert, *CALPHAD* **34**, 487 (2010).
- ¹³M. Palumbo, T. Abe, C. Kocer, H. Murakami, and H. Onodera, *CALPHAD* **34**, 495 (2010).
- ¹⁴R. McCormack, D. de Fontaine, C. Wolverton, and G. Ceder, *Phys. Rev. B* **51**, 15808 (1995).
- ¹⁵M. Asta, A. Ormeci, J. M. Wills, and R. C. Albers, *Mater. Res. Soc. Symp. Proc.* **364**, 157 (1995).
- ¹⁶R. McCormack and D. de Fontaine, *Phys. Rev. B* **54**, 9746 (1996).
- ¹⁷P. E. A. Turchi, V. Drchal, J. Kudrnovsky, C. Colinet, L. Kaufman, and Z.-K. Liu, *Phys. Rev. B* **71**, 094206 (2005).
- ¹⁸M. Sluiter, M. Takahashi, and Y. Kawazoe, *J. Alloys Comp.* **248**, 90 (1997).
- ¹⁹N. Motta and N. E. Christensen, *Phys. Rev. B* **43**, 4902 (1991).
- ²⁰B. P. Burton, J. E. Osburn, and A. Pasturel, *Phys. Rev. B* **45**, 7677 (1992).
- ²¹G. Kresse and J. Hafner, *Phys. Rev. B* **47**, 558 (1993).
- ²²G. Kresse and J. Furthmüller, *Comput. Mater. Sci.* **6**, 15 (1996).
- ²³G. Kresse and J. Furthmüller, *Phys. Rev. B* **54**, 11169 (1996).
- ²⁴J. P. Perdew in *Electronic Structures of Solids*, edited by P. Ziesche and H. Eshrig (Akademie Verlag, Berlin, 1991), p. 11.
- ²⁵H. J. Monkhorst and J. D. Pack, *Phys. Rev. B* **13**, 5188 (1976).
- ²⁶G. Kresse [<http://cms.mpi.univie.ac.at/vasp-workshop/slides/pseudopdatabase.pdf>].
- ²⁷P. E. Blochl, O. Jepsen, and O. K. Andersen, *Phys. Rev. B* **49**, 16223 (1994).
- ²⁸A. van de Walle and G. Ceder, *Rev. Mod. Phys.* **74**, 11 (2002).
- ²⁹See supplemental material at [<http://link.aps.org/supplemental/10.1103/PhysRevB.83.144109>], where all calculated energies, magnetizations, lattice parameters, and volumes are reported.
- ³⁰J. S. Kasper *Atomic and Magnetic Ordering in Transition Metal Structure in Theory of Alloy Phases* (ASM, Cleveland, 1956), p. 264.
- ³¹J. S. Kasper and R. M. Waterstrat, *Acta Crystallogr.* **9**, 289 (1956).
- ³²J.-M. Joubert, *Prog. Mater. Sci.* **53**, 528 (2008).
- ³³B. Seiser, R. Drautz, D. G. Pettifor, *Acta Mater.* **59**, 749 (2011).
- ³⁴I. V. Ametov, S. F. Dunaev, E. M. Slyusarenko, and A. V. Peristy, *Moscow Univ. Chem. Bull.* **45**, 1 (1990).
- ³⁵H. L. Lukas, S. G. Fries, and B. Sundman, *Computational Thermodynamics* (Cambridge University Press, Cambridge, 2007).
- ³⁶See [<http://www.thermocalc.se>].
- ³⁷T. Massalski, editor, *Binary Alloy Phase Diagrams*, 2nd ed. (ASM International, Materials Park, 2007).
- ³⁸S. Saito, K. Kurokawa, S. Hayashi, T. Takashima, and T. Narita, *J. Jpn. Inst. Met.* **72**, 132 (2008).
- ³⁹S. Saito, K. Kurokawa, S. Hayashi, T. Takashima, and T. Narita, *J. Jpn. Inst. Met.* **71**, 608 (2007).
- ⁴⁰E. M. Slyusarenko, A. V. Peristy, E. Yu. Kerimov, M. V. Sofin, and D. Yu. Skorbov, *J. Alloys Compd.* **264**, 180 (1998).
- ⁴¹W. Huang and Y. A. Chang, *J. Alloys Compd.* **274**, 209 (1998).